J. Fluid Mech. (1996), vol. 319, pp. 67–76

A generalized stability criterion for resonant triad interactions

By CARSON C. CHOW[1], DIANE HENDERSON[2] AND HARVEY SEGUR[3]

[1] NeuroMuscular Research Center, Boston University, Boston, MA 02215, USA
[2] Department of Mathematics, Penn State University, University Park, PA 16802, USA
[3] Program in Applied Mathematics, University of Colorado, Boulder, CO 80309-0526, USA

(Received 12 September 1995 and in revised form 20 February 1996)

It is well known that in any conservative system that admits resonant triad interactions, a uniform (test) wavetrain that participates in a single triad is unstable if it has the highest frequency in the triad, and neutrally stable otherwise. We show that this result changes significantly in the presence of coupled triads: with coupling, the test wave can be unstable to a high-frequency perturbation. The coupling sends energy from the (weak) high-frequency source into particular low-frequency waves that grow even though they had zero amplitudes initially. This mechanism thereby selects these low-frequency waves from the spectrum of low-frequency waves available for triad interactions. Moreover, the instability persists in the presence of weak damping, provided the wave amplitudes exceed two thresholds. First, the initial amplitude of the test wavetrain must be large enough for the instability to dominate the damping. Secondly, the (small) initial amplitudes of the high-frequency perturbations must exceed a threshold in order for the low-frequency waves to grow to a prescribed amplitude.

1. Introduction

The purpose of this paper is to examine the stability of a monochromatic wavetrain to resonant triad interactions. A well-known result is that if a monochromatic wavetrain, which we call a 'test wave', participates in a resonant triad involving itself and two perturbative waves in a conservative system, then the test wave is unstable to the perturbations if it has the highest frequency in the triad, and neutrally stable otherwise. This result is known in plasma physics as the 'decay instability' (e.g. Tsytovich 1970). It arises in many other systems as well, including electrical engineering (e.g. Louisell 1960), geophysics (e.g. Hasselmann 1967) and nonlinear optics (e.g. Harper & Wherrett 1975). It has been corroborated in laboratory experiments (e.g. McEwan 1971), and in (oceanographic) field observations (e.g. Neshyba & Sobey 1975). (In the degenerate case of second harmonic resonance, this classical stability result breaks down; e.g. McGoldrick 1965.) For general discussions of resonant triad interactions in various physical contexts, see Bers (1972) or Craik (1984). See Hammack & Henderson (1993) for a recent review of resonant triad interactions among surface water waves.

The usual result considers the stability of a test wave within a single resonant triad. Nevertheless, many systems that admit resonant triads also admit multiple triad interactions, so that a given wave can participate in several triads simultaneously, and distinct triads can be coupled to each other through these multiple interactions. In this paper, we generalize the usual result by investigating the stability of a test wave that participates in a system of coupled triads. In §2 we show that the test wave is unstable to perturbations at lower frequencies (as it is in a single triad), but that it can also be unstable to a perturbation at a higher frequency (which cannot occur in a single triad). The coupled triads provide a mechanism to send energy from a (weak) high-frequency perturbation into particular low-frequency waves that grow even though they had zero amplitudes initially.

One effect of this mechanism occurs when a test wave has the highest frequency in a continuum of triads, so that a continuum of low-frequency waves can potentially grow at the expense of the test wave. In this case a small, monochromatic, high-frequency energy source can determine which of the unstable modes actually do grow. In other words, coupled resonant triads can provide a selection mechanism to choose among a continuum of unstable wave modes.

This work was motivated by experiments on capillary–gravity waves by Henderson & Hammack (1987; Part 1) and Perlin, Henderson & Hammack (1990, Part 2). In each experiment, they generated a test wave that was unstable to a continuum of waves at lower frequencies, and they expected to see energy transferred over a continuum of frequencies, as predicted by Simmons (1969). Instead they observed that a particular low-frequency triad was selected for each unstable test wave. The selected triad was found to be excited by a high-frequency perturbation at 60 Hz from the digital-to-analog converter in the computer that ran the wavemaker. The selection of a particular low-frequency triad for a given test wave frequency was empirically explained and predicted by considering it to be the consequence of a sequence of triad interactions that began with the 60 Hz perturbation's interacting with the test wave. Upon discovering this perturbation as the cause of the low-frequency triads, the authors replaced it with their own high-frequency perturbations at various frequencies and correctly predicted which low-frequency triads would be selected. However, they noted that according to the usual stability result, the test waves were considered stable to high-frequency perturbations, so that neither the 60 Hz noise nor their imposed high-frequency noise was expected to have affected the evolution of the test wavetrains.

In §2 we consider the sequence of triad interactions discussed in Part 2 as a system of three coupled resonant triad interactions involving seven distinct wavetrains. We will show that this 7-wave model provides a selection mechanism for the observed low-frequency triads without violating the usual stability result. Instead, it generalizes this result to show that through triad coupling, a test wavetrain can be unstable to high-frequency perturbations. The model also shows that the instability can persist in the presence of viscous damping. Analysis of the seven-wave model in §2 shows that the high-frequency perturbations do not grow larger than their initial sizes, and identifies two threshold amplitudes necessary for the growth of the low-frequency waves. First, all wave amplitudes decay unless the test wave has a large enough amplitude for the instability to dominate viscous damping. Secondly, the (small) initial amplitudes of the high-frequency perturbations must exceed a threshold in order for the low-frequency waves to grow to a prescribed amplitude. Correspondingly, given the initial amplitude of the high-frequency noise waves, the second threshold provides a maximum amplitude for the unstable low-frequency waves. The analysis also predicts the approximate location of maximum growth of the low-frequency waves.

The threshold amplitudes identified by this model are qualitatively consistent with the experimental results reported in Parts 1 and 2. Quantitative comparison with those experiments is inconclusive because the second threshold involves amplitudes of high-frequency waves, which were not measured.

Finally, we note that the seven-wave model is weakly nonlinear, so the amplitude of the test wave is assumed to be small, and the perturbating waves, even smaller. If the test wave is large enough to interact nonlinearly with itself, then this model is inadequate. A generalized seven-wave model that includes nonlinear interactions of the test wave with itself is discussed in the Appendix. A preliminary analysis of this model shows that the high-frequency perturbations remain small in the generalized model, and that the instability discussed in this paper persists.

2. The 7-wave equations

The theoretical model proposed in Part 2 for a particular test wave, e.g. one with a frequency of 25 Hz, can be summarized as follows. In the experiments described in Parts 1 and 2, capillary–gravity waves were generated in deep water at 25 Hz; the electronic equipment, operating at 60 Hz, generated water waves of very small amplitude at 60 Hz, and these waves fed a small amount of energy into a 35 Hz wave through a resonant triad. Next, the 35 Hz wave interacted with a 25 Hz wave through a second triad, to create a 10 Hz wave. Then the 10 Hz wave interacted with a 25 Hz wave in a third triad to create a 15 Hz wave. However, this 25 Hz wave had the highest frequency in the $\{10, 15, 25\}$ triad, so the 10 and 15 Hz waves grew at the expense of the 25 Hz wave, according to the usual stability result. In this way, the weak 60 Hz wave selected the $\{10, 15, 25\}$ triad from the continuum of triads available. In this scenario, the sequence of triads occurred at successively higher order in nonlinearity. The wavevectors had the proper directions for satisfying the kinematic resonance conditions owing to a directional instability (investigated by Perlin & Hammack 1991).

The model we now present is based on this earlier model. However, the current model is quantitative, rather than conceptual. It treats the triads as a coupled system, rather than sequentially, so that all of the triad interactions occur at quadratic order of nonlinearity. Further, it allows viscous damping to compete with the instability, as occurs in the actual experiments.

2.1. *Amplitude equations*

Several two-timing procedures are known to derive equations for the slow evolution of the complex amplitudes of monochromatic wavetrains interacting in resonant triads. Zakharov (1968) and Simmons (1969) apply two of these procedures specifically to inviscid capillary-gravity waves. The resulting slow equations for the seven interacting wave amplitudes constitute a Hamiltonian system, with Hamiltonian

$$H = A\sigma_1\sigma_2\sigma_3(a_1a_2a_3 + a_1^*a_2^*a_3^*) + B\sigma_2\sigma_4\sigma_5(a_2a_4a_5 + a_2^*a_4^*a_5^*) + \Gamma\sigma_5\sigma_6\sigma_7(a_5a_6a_7 + a_5^*a_6^*a_7^*), \quad (1a)$$

where $a_j(t)$ is the complex amplitude of the jth wave mode, $a_j^*(t)$ is its complex conjugate with $\sigma_j a_j^*(t)$ its conjugate variable in the Hamiltonian system, $\{A, B, \Gamma\}$ are positive, real-valued interaction coefficients, and $\sigma_j = \pm 1$. Precise values for the interaction coefficients can be inferred from Zakharov (1968) or Simmons (1969). We omit their values here; however, they are essential for a comparison with experimental results. The σ_j arise from the kinematic resonance conditions. The conditions for the first triad are

$$\sigma_1\omega_1 + \sigma_2\omega_2 + \sigma_3\omega_3 = 0, \quad (1b)$$

$$\sigma_1\boldsymbol{k}_1 + \sigma_2\boldsymbol{k}_2 + \sigma_3\boldsymbol{k}_3 = 0, \quad (1c)$$

$$\omega_j = \omega_j(\boldsymbol{k}_j), \quad (1d)$$

where $\omega_j > 0$. Similar conditions hold for the other two triads.

To relate this Hamiltonian with the experiments of Parts 1 and 2, we identify: $a_6 \leftrightarrow$ 25 Hz (the test wave), $a_1 \leftrightarrow 60$ Hz (the high-frequency source), $a_2 \leftrightarrow 35$ Hz, $a_3 \leftrightarrow 25$ Hz, $a_4 \leftrightarrow 25$ Hz, $a_5 \leftrightarrow 10$ Hz, and $a_7 \leftrightarrow 15$ Hz. Waves a_3, a_4, and a_6 all have the same frequency (25 Hz), but they must have different wavevectors, in order to satisfy the kinematic resonance conditions. We *assume* that the mechanical means to generate a test wave at 25 Hz also generates perturbative waves in other directions at 25 Hz. Thus, the kinematic conditions on wavevectors (1*c*) are satisfied, and a_3 and a_4 are present initially, but are very weak.

The theory is for waves with small amplitudes, so that there is a small parameter $\delta \ll 1$ that is a measure of weak nonlinearity. This parameter has been scaled out of the amplitudes in (1), so that it does not explicitly appear in the resulting evolution equations, in which derivatives are understood to be with respect to a slow time.

The Hamiltonian in (1) implies a dynamical system consisting of ordinary differential equations. Alternatively, one could derive a system of coupled partial differential equations, for which (1) is replaced by a two-dimensional spatial integral. We present the ODE system in order to simplify the presentation. It can be obtained from the PDE system by denying all spatial variation of the wave amplitudes, or by denying temporal variation and permitting spatial variation only in the direction perpendicular to the paddle (i.e. in the direction of propagation of the test wave). The interaction coefficients for the two versions are different; both sets can be obtained from the references cited above.

The corresponding system of evolution equations is non-dissipative, but viscous damping can be added following, for example, Bers (1972) or Craik (1984, p. 152). The result is a system of seven coupled, complex ODEs of the form:

$$a_1' = -\nu_1 a_1 - \mathrm{i} a_2^* a_3^*, \tag{2a}$$

$$a_2' = -\nu_2 a_2 + \mathrm{i} a_3^* a_1^* - \mathrm{i}\beta a_4^* a_5^*, \tag{2b}$$

$$a_3' = -\nu_3 a_3 + \mathrm{i} a_1^* a_2^*, \tag{2c}$$

$$a_4' = -\nu_4 a_4 + \mathrm{i}\beta a_5^* a_2^*, \tag{2d}$$

$$a_5' = -\nu_5 a_5 + \mathrm{i}\beta a_2^* a_4^* + \mathrm{i}\gamma a_6^* a_7^*, \tag{2e}$$

$$a_6' = -\nu_6 a_6 - \mathrm{i}\gamma a_7^* a_5^*, \tag{2f}$$

$$a_7' = -\nu_7 a_7 + \mathrm{i}\gamma a_5^* a_6^*, \tag{2g}$$

where $\nu_j \geqslant 0$, and time has been rescaled by A. The constants, $\beta = B/A$ and $\gamma = \Gamma/A$, measure the relative strengths of the nonlinear coupling in triads 2 and 3 as compared to that in triad 1. The choice of signs for the nonlinear terms in (2) corresponds to choosing σ_j in (1) such that $\omega_1 = \omega_2 + \omega_3, \omega_2 = \omega_4 + \omega_5, \omega_6 = \omega_5 + \omega_7$. This choice is consistent with the scenario of triad interactions discussed above for the experiments of Parts 1 and 2.

2.2. *Amplitude bounds*

To obtain bounds for the amplitudes, assume that $\nu_1 \geqslant \nu_2 \geqslant \nu_3 \geqslant \nu_4 \geqslant \nu_6 \geqslant \nu_7 \geqslant \nu_5 \geqslant 0$. This choice is consistent with the experiments of Parts 1 and 2; the analysis that follows can be modified easily for other choices. In the absence of damping ($\nu_j = 0$ for $j = 1$–7) equations (2) admit four Manley–Rowe relations (Manley & Rowe 1956), resulting in four conserved quantities in addition to the (conserved) Hamiltonian. With non-zero damping these four quantities decay as

$$|a_1|^2 + |a_3|^2 \leqslant C_1 \exp(-2\nu_3 t), \tag{3a}$$

$$|a_6|^2+|a_7|^2 \leqslant C_2 \exp(-2\nu_7 t), \tag{3b}$$

$$|a_1|^2+|a_2|^2+|a_4|^2 \leqslant C_3 \exp(-2\nu_4 t), \tag{3c}$$

$$-|a_5|^2+|a_7|^2+|a_4|^2 \leqslant C_4 \exp(-2\nu_7 t), \tag{3d}$$

where C_j are constants that can be obtained from the initial conditions. The bound in (3d) applies when the left-hand side is positive at time $t = 0$. The initial conditions corresponding to the experiments are consistent with this restriction; they are:

$$\left.\begin{array}{lll} |a_6(0)| = C = O(1), & & \\ |a_1(0)| = \epsilon_1 = O(\epsilon), & |a_3(0)| = \epsilon_2 = O(\epsilon), & |a_4(0)| = \epsilon_3 = O(\epsilon), \\ |a_2(0)| = o(\epsilon), & |a_5(0)| = o(\epsilon), & |a_7(0)| = o(\epsilon), \end{array}\right\} \tag{4}$$

where $\epsilon \ll 1$. These initial conditions correspond to a test wave with amplitude a_6 that contains most of the initial energy, a perturbation a_1, with a higher frequency than that of the test wave, a perturbation a_2, with a higher frequency than that of the test wave and with an amplitude that can be initially zero, perturbations a_3 and a_4, which have the same frequency of the test wave but different wavevectors, and waves a_5 and a_7 with lower frequencies than that of the test wave and with amplitudes that can be initially zero. Recall that in both (2) and (4), the measure of weak nonlinearity, δ, has been scaled out so that a_6 is $O(1)$ rather than $O(\delta)$, a_1, a_3 and a_4 are $O(\epsilon)$ rather than $O(\delta\epsilon)$, and a_2, a_5, and a_7 are $o(\epsilon)$ rather than $o(\delta\epsilon)$.

From these initial conditions and from (2) (with $t = 0$), the constants are found to be

$$\left.\begin{array}{l} C_1 = K_1 \epsilon^2, \\ C_2 > 0, \\ C_3 = K_3 \epsilon^2, \\ C_4 = K_4 \epsilon^2, \end{array}\right\} \tag{5}$$

where $K_j \geqslant 0$, and $K_j = O(1)$. Then for all time the perturbation amplitudes are bounded such that

$$|a_1(t)| \leqslant \epsilon (K_1)^{1/2} \exp(-\nu_3 t), \tag{6a}$$

$$|a_2(t)| \leqslant \epsilon (K_3)^{1/2} \exp(-\nu_4 t), \tag{6b}$$

$$|a_3(t)| \leqslant \epsilon (K_1)^{1/2} \exp(-\nu_3 t), \tag{6c}$$

$$|a_4(t)| \leqslant \epsilon (K_3)^{1/2} \exp(-\nu_4 t). \tag{6d}$$

Thus all of the high-frequency waves remain small, decaying exponentially from initially small amplitudes. In addition,

$$|a_7(t)|^2 \leqslant |a_5(t)|^2 + Z(t), \tag{6e}$$

where

$$|Z(t)| \leqslant \epsilon^2 K_4 \exp(-2\nu_7 t). \tag{6f}$$

Thus, $a_7(t)$ cannot grow larger than $O(\epsilon)$ unless $a_5(t)$ also grows.

2.3. *Solution for small times*

To determine whether or not $a_5(t)$ grows, differentiate (2e) and substitute in (2b, d, f, g) to obtain

$$a_5'' + (\nu_5+\nu_6+\nu_7)\, a_5' + \nu_5(\nu_6+\nu_7)\, a_5 = (\gamma^2 |a_6|^2 + \beta^2 |a_2|^2 - \gamma^2 |a_7|^2 - \beta^2 |a_4|^2)\, a_5 + \beta a_1 a_3 a_4^* + \mathrm{i}\beta(\nu_7 - \nu_2 + \nu_6 - \nu_4)\, a_2^* a_4^*. \tag{7}$$

The terms on the right-hand side of (7) are bounded, using (6), as follows:

$$|a_1 a_3 a_4^*| \leqslant \epsilon^3 K_1 (K_3)^{1/2} \exp(-(2\nu_3+\nu_4)t), \quad (8a)$$

$$|\mathrm{i}(\nu_7-\nu_2+\nu_6-\nu_4)\, a_2^* a_4^*| \leqslant \epsilon^2 (K_1 K_3)^{1/2} \exp(-(\nu_3+\nu_4)t)\,|\nu_7-\nu_2+\nu_6-\nu_4|, \quad (8b)$$

and

$$|\beta^2(|a_2|^2-|a_4|^2)| \leqslant 2\epsilon^2\beta^2 K_3 \exp(-2\nu_4 t) \quad (8c)$$

At early times a_5 and a_7 are still small (because $\epsilon \ll 1$), and $|a_6(t)|^2 \approx C^2 \exp(-2\nu_6 t)$, so (7) can be approximated by a forced linear equation

$$A_5''+(\nu_5+\nu_6+\nu_7)A_5'+\nu_5(\nu_6+\nu_7)A_5 = C^2\gamma^2 \exp(-2\nu_6 t)A_5+f(t), \quad (9)$$

where $A_5(t)$ approximates $a_5(t)$ for early times, and $f(t)$ can be considered a known forcing function that arises from the perturbation waves. The forcing term has a bound that is uniformly valid in time of $f(t) = O(\epsilon^2 \exp(-(\nu_3+\nu_4)t))$ according to (8). However, in the system of interest here, $a_2(0) = 0$ so that at early times, $f(t) = O(\epsilon^3 \exp(-(2\nu_3+\nu_4)t))$.

To simplify (9), we assume that $\nu_5 = \nu_7$. This assumption is reasonable for the experiments of Parts 1 and 2. Results of numerical integrations of (2) using the values of ν_5 and ν_7 from Parts 1 and 2 support the predictions of the linearized analysis. Setting

$$A_5 = \xi \exp(-\nu_5 t), \quad (10)$$

and using $\nu_5 = \nu_7$, (9) becomes

$$\xi''+\nu_6\xi' = C^2\gamma^2 \exp(-2\nu_6 t)\,\xi+f(t)\exp(\nu_5 t). \quad (11)$$

The homogeneous part of (11), with $f = 0$, has solutions

$$\{\exp(-(C\gamma/\nu_6)\exp(-\nu_6 t)), \exp((C\gamma/\nu_6)\exp(-\nu_6 t))\};$$

this result can also be obtained from Miles (1984). Using the homogeneous solutions, one finds the solution of (11) via variation of parameters:

$$\xi(t) = A\exp\left(\frac{C\gamma}{\nu_6}\exp(-\nu_6 t)\right)+B\exp\left(-\frac{C\gamma}{\nu_6}\exp(-\nu_6 t)\right)$$
$$+\frac{1}{2C\gamma}\int_0^t\left[\exp\left[-\frac{C\gamma}{\nu_6}(\exp(-\nu_6 t)-\exp(-\nu_6\tau))\right]\right.$$
$$\left.-\exp\left[\frac{C\gamma}{\nu_6}(\exp(-\nu_6 t)-\exp(-\nu_6\tau))\right]\right]\exp((\nu_6+\nu_5)\tau)f(\tau)\,\mathrm{d}\tau, \quad (12)$$

where A and B involve the initial amplitudes and growth rates of ξ. Here we take $C\gamma > 0$ without loss of generality. Then the first term in (12) decays in time. The second term grows at an approximately exponential rate for a while. This is the usual instability: with no high-frequency perturbations ($f(t) \equiv 0$), the low-frequency triad in (2) is not affected by the other triads; the low-frequency modes of this triad (a_5 and a_7) grow if both are small initially and do not grow if both vanish initially.

To investigate the growth of $a_5(t)$ if both $a_5(0)$ and $a_7(0)$ vanish (i.e. if both low-frequency waves are initially zero), we take $B = 0$ in (12). For the integral in (12) to grow appreciably, we need

$$\frac{C\gamma}{\nu_6} \gg 1. \quad (13)$$

This is the first of two cut-off criteria. It says that the test wave must have an initial amplitude C such that growth due to nonlinearity dominates decay due to viscous damping. With $f(t)$ uniformly bounded and small, the contribution from the second term in the integral is uniformly bounded; it goes to zero as $C\gamma/\nu_6 \rightarrow \infty$. The dominant contribution of the integral comes from the first term, in a small neighbourhood of $\tau = 0$.

The maximum growth of A_5 is obtained by differentiation using (10) and (12), evaluating the forcing term, $f(t)$ at $\tau = 0$, assuming (13) holds, and considering the limit of τ small. The forcing term contains the $O(\epsilon^3)$, $a_1 a_3 a_4^*$ term and the $O(\epsilon^2)$, $a_2^* a_4^*$ term. In the experiments of Parts 1 and 2, $a_2(0) = 0$, so that $f(0) = \beta\epsilon_1 \epsilon_2^2$. The time for maximum growth, then, is

$$t^* = \ln\left(\frac{C\gamma}{\nu_5}\right)\bigg/\nu_6, \qquad (14)$$

and the maximum amplitude is

$$|A_5|_{\max} \approx \frac{\left[\dfrac{\nu_5}{C\gamma e}\right]^{(\nu_5/\nu_6)} \beta\epsilon_1 \epsilon_2 \epsilon_3 \exp\left(C\gamma/\nu_6\right)}{2C^2\gamma^2}. \qquad (15)$$

This amplitude provides a second cut-off for the growth of the low-frequency triad in (2). It says that the initial amplitudes of the perturbative waves, ϵ_1 and ϵ_2, have to be large enough to allow A_5 to grow to an observable size.

The above linearized analysis of the seven-wave model shows that a high-frequency perturbation can destabilize a test wave through coupled triads, as it cannot for a single triad. The amplitudes of the high-frequency perturbations do not exceed their initial sizes; rather, they channel energy from the test wave to the low-frequency waves. The growth within the low-frequency triads depends on two cut-offs: the first (13) is a viscous threshold for the initial amplitude of the test wave; the second (15) is a constraint on the initial amplitudes of the perturbations.

This analysis is for a particular coupling of seven waves chosen to describe the experiments of Parts 1 and 2. A similar analysis follows for other systems of coupled triads. Instability will occur if and only if: (i) the low-frequency waves are members of a triad with the test wave; (ii) one of the low-frequency waves is coupled to a higher-frequency perturbation through a second triad interaction; and (iii) that higher-frequency perturbation is coupled to an additional high-frequency perturbation (the 60 Hz noise in the present model) either through the second triad or through coupling within another triad. The direct coupling of a low-frequency wave to a high-frequency perturbation is the selection mechanism that chooses that particular low-frequency wave over the continuum of possibilities. The further, direct coupling with the test wave is the mechanism that provides the energy that allows the low-frequency waves to grow.

These conclusions have been based on the solution of (9), but a related analysis shows that the solution of (9) does indeed remain close to that of (7) for early times. The behaviour of the solution of (7) is similar to that of (9), except that the time in (14) should be reinterpreted as a lower bound for the time of maximum growth. We have not analysed (7) in detail, because our main objective was to describe the instability, which can be seen from (9).

Numerical integrations of (2) with $\gamma = \beta = 1$ and without damping, i.e. $\nu_j = 0$, are presented in figure 1. The amplitudes as functions of time are shown on the same scale for each wave to show the instability mechanism provided by the coupled triad model.

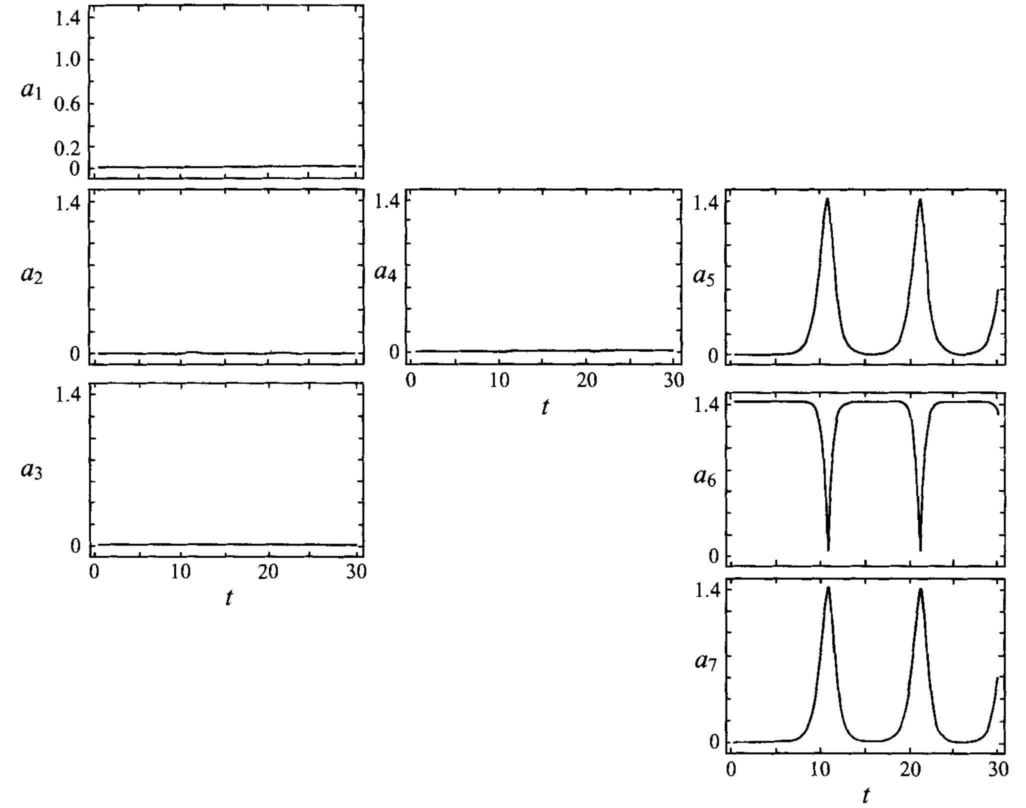

FIGURE 1. Wave amplitudes as a function of time from (2) with $\nu_j = 0$ and $\gamma = \beta = 1$. The initial conditions are $a_1(0) = a_3(0) = a_4(0) = 0.01 + i0.01$, $a_2(0) = a_5(0) = a_7(0) = 0$, and $a_6(0) = 1 + i1$.

The high-frequency waves do not grow; their amplitudes are inconsequential. Nevertheless, the low-frequency waves that both started out with zero amplitude grow and dominate the wavefield evolution.

Finally, we compare the predictions of this theory with the experimental results from Parts 1 and 2 that motivated it. Selective amplification of low-frequency waves was observed in six of the eight experiments that involved test waves at 25 Hz and a high-frequency source at 60 Hz. Measurements of ϵ_2 in the experiments were not available, so quantitative comparisons are inconclusive. We find that the predictions are in qualitative agreement, but quantitative disagreement with the experiments. In particular, agreement was qualitative because we have found a single value of ϵ_2 (and estimated values of C and ϵ_1) such that (15) predicts measurable growth in all six experiments in which selective growth was observed, and no measurable growth in the other two experiments; that is, an ϵ_2 can be found so that the predictions of stability or instability implied from (15) agree with observations of stability or instability observed in the experiments. The comparison was in quantitative disagreement because the seven-wave model's predictions of the values of maximum amplitude, from (15), and their locations, from (14), underestimate those measured in the experiments. We speculate that other mechanisms in addition to the one discussed herein are responsible for the quantitative disagreement. Because the experiments that motivated this analysis were not designed to test its predictions, we feel that additional experiments are required for a quantitative test of the theory. Regardless, coupled triads are possible in many systems, including nonlinear optics, plasma physics, electrical engineering, surface waves, and geophysics: thus the seven-wave model described herein provides a mechanism by which a test wave may become unstable to high-frequency noise, in contrast to predictions from the usual stability considerations.

We are grateful to Joe Hammack for useful discussions and to the Mathematical Sciences Research Institute (supported in part by NSF grant DMS-9022140) where discussions on this work began. This work was supported in part by the NSF grants DMS-9304390, DMS-9257456, DMS-9022140, and by the David and Lucile Packard Foundation.

Appendix

Here we add cubic nonlinearity to the evolution equation for the test wavetrain, which is the only one of the seven waves to start out with an initially finite amplitude. Thus the seven-wave equations are modified so that (2*f*) becomes

$$\dot{a}_6 = -\nu_6 a_6 - \mathrm{i} a_7^* a_5^* + \mathrm{i}M|a_6|^2 a_6, \tag{16}$$

where M is a real-valued constant. With the addition of the cubic term, (3)–(5) remain unchanged. Thus, the cubic nonlinear correction does not change the result that the high-frequency perturbations remain small for all time. Equation (7) for a_5 is modified so that the term $(\nu_6+\nu_7)$ is replaced by $(\nu_6+\nu_7+\mathrm{i}M|a_6|^2)$ in all three of its occurrences. The approximation for a_6 (under equation (8)) still applies so that in (9) the modification due to cubic nonlinearity is that $(\nu_6+\nu_7)$ is replaced by $(\nu_6+\nu_7+\mathrm{i}MC^2\exp(-2\nu_6 t))$ in both places where it occurs. We note that if we use the dimensional values for ν_6, ν_7, M (e.g. Perlin & Hammack 1991), and $a_6(0)$ that correspond to the experiments of Parts 1 and 2, then the self-interaction term is about three orders of magnitude smaller than the damping terms initially and is not expected to change the threshold predictions to a measurable extent.

REFERENCES

Bers, A. 1972 Linear waves and instabilities. In *Plasma Physics – Les Houches* (ed. C. De Witt & J. Peyraud), pp. 117–215. Gordon and Breach, New York, 1975).

Craik, A. D. D. 1984 *Wave Interactions and Fluid Flows*. Cambridge University Press.

Hammack, J. L. & Henderson, D. M. 1993 Resonant interactions among surface water waves. *Ann. Rev. Fluid Mech.* **25**, 55–97.

Harper, P. G. & Wherrett, B. S. 1975 *Nonlinear Optics*. Academic Press.

Hasselmann, K. 1967 A criterion for nonlinear wave stability. *J. Fluid Mech.* **30**, 737–739.

Henderson, D. & Hammack, J. 1987 Experiments on ripple instabilities. Part 1. Resonant triads. *J. Fluid Mech.* **184**, 15–41.

Louisell, W. H. 1960 *Coupled Mode and Parametric Electronics*. Wiley.

McEwan, A. D. 1971 Degeneration of resonantly-excited standing internal waves. *J. Fluid Mech.* **50**, 431–448.

McGoldrick, L. F. 1965 Resonant interactions among capillary–gravity waves. *J. Fluid Mech.* **21**, 305–331.

Manley, J. M. & Rowe, H. E. 1956 Some general properties of nonlinear elements – Part I. General energy relations. *Proc. I.R.E.* **44** 904–913.

Miles, J. W. 1984 On damped resonant interactions. *J. Phys. Oceanogr.* **14**, 1677–1678.

Neshyba, S. & Sobey, E. J. C. 1975 Vertical cross coherence and cross bispectra between internal waves measured in a multiple-layered ocean. *J. Geophys. Res.* **80**, 1152–1162.

PERLIN, M. & HAMMACK, J. 1991 Experiments on ripple instabilities. Part 3. Resonant quartets of the Benjamin–Feir type. *J. Fluid Mech.* **229**, 229–268.

PERLIN, M., HENDERSON, D. & HAMMACK, J. 1990 Experiments on ripple instabilities. Part 2. Selective amplification of resonant triads. *J. Fluid Mech.* **219**, 51–90.

SIMMONS, W. F. 1969 A variational method for weak resonant interactions. *Proc. R. Soc. Lond.* A **309**, 551–575.

TSYTOVICH, V. N. 1970 *Nonlinear Effects in Plasma.* Trans. from Russian by J. S. Wood. Plenum Press.

ZAKHAROV, V. E. 1968 Stability of periodic waves of finite amplitude on the surface of a deep fluid. *J. Appl. Mech. Tech. Phys.* **9**, 190–194.